January 2001 • NREL/CP-500-29132

Conference Paper

Wind Turbine Wake Measurements in the Operating Region of a Tail Vane

S. Larwood

Presented at the 39th American Institute of Aeronautics and Astronautics, Inc. (AIAA) Aerospace Sciences Meeting
Reno, Nevada
January 8–11, 2001

National Renewable Energy Laboratory

1617 Cole Boulevard
Golden, Colorado 80401-3393

NREL is a U.S. Department of Energy Laboratory
Operated by Midwest Research Institute • Battelle • Bechtel

Contract No. DE-AC36-99-GO10337

WIND TURBINE WAKE MEASUREMENTS IN THE OPERATING REGION OF A TAIL VANE

Scott Larwood
National Wind Technology Center
National Renewable Energy Laboratory
Golden, Colorado
scott_larwood@nrel.gov

ABSTRACT

In conjunction with the National Renewable Energy Laboratory's (NREL's) Unsteady Aerodynamics Experiment (UAE) at NASA Ames, we measured the wake of an upwind 10-meter (m) diameter wind turbine in the typical region of a tail vane. The experiment was performed in a 24.4-by-36.6-m wind tunnel. We placed two sonic anemometers 0.58 rotor diameters downwind of the rotor at hub height. One was positioned nominally behind the nacelle at 9% radius and the second was placed 2-m outboard at 49% radius. The tunnel wind speed was varied from 5 to 25 meters per second (m/s) and the turbine rotor speed was held at 72 revolutions per minute (rpm). We varied yaw from 0º to 60º. The data showed unsteadiness in the wake due to the nacelle wake. Also, the unsteadiness increased with the onset of blade stall. The axial induction factor in the wake showed that the turbine was operating within the windmill brake state of actuator disk momentum theory. Little variation in unsteadiness was shown under yawed conditions. We also discovered that lateral velocity behind the nacelle was negative and would result in an unfurling normal force on a tail vane. The vertical velocity was shown to change sign under yawed conditions, conceivably as a result of the opposing blade root vortex.

INTRODUCTION

Besides providing the best position for a company's logo, the tail vane has been serving as a passive control device on wind turbines for more than a century. Small turbines manufactured today continue to incorporate the tail vane as a means of aligning the rotor to maximize energy capture. The tail vane delays furling by keeping the rotor aligned with the wind until the furling moment on the rotor is sufficient to overcome the gravity preload on the tail vane hinge. Researchers at NREL's Small Turbine Program have displayed new interest in the physics of furling.

Small Turbine Program

The United States Department of Energy (DOE) embarked on a program in 1995 to stimulate the application of advanced technology in the portion of the industry that serves markets requiring wind turbines in 5- to 40-kilowatt range.[1] All of the prototype designs in this program use furling as a passive control mechanism to minimize overshoots in both power and loads at high wind speeds. Furling occurs when the rotor yaws out of the wind with the tail remaining nominally in the undisturbed wind direction. The yawed rotor presents a reduced effective area, thus lowering rotor speed and power.

Experiments under the Small Turbine Program were performed in the past few years to correlate field-test data with models of turbine furling.[2] Researchers intended to use these models to assist in furling turbine design, and to determine loads for potential certification under International Electrotechnical Commission standards. One area of uncertainty in these models was in tail vane aerodynamics.

Tail Region Aerodynamic Modeling

Tail aerodynamic models found in the literature are simplified adaptations of momentum theory.[3] Below are three models of the velocity in the region of the tail:

1. Ackerman,[4] near wake approximation: $U_{wake} = U \times (1 - a)$
2. Chen,[5] undisturbed wind speed: $U_{wake} = U$
3. Eggers,[2] far wake: $U_{wake} = U \times (1 - 2 \times a)$

where:

U_{wake} = the axial velocity of the wake
U = the undisturbed wind speed
a = the axial induction factor at the rotor disc

These models only determine the axial velocity. We obtained the axial induction factor at the rotor disk from the rotor aerodynamic model.

Model comparisons with small turbine yawing and furling field-test data showed discrepancies in the tail normal-force predictions. We suggested, based on these discrepancies and due to a lack of wake data, that velocity measurements be made in the region of a tail vane to help with aerodynamic modeling efforts.

Wake Measurement Studies

Past wake studies have focused either on correlation with rotor aerodynamic models or on wake impacts on turbine array operations. For rotor aerodynamic modeling efforts, measurements were made within two chord lengths of the rotor. For array studies, measurements were obtained in the region greater than two rotor diameters downstream. These measurements are out of the typical range of a tail vane, usually placed 0.5 to 0.7 diameters downwind of the rotor. However, some of these data in the literature can be of qualitative use in the study of tail aerodynamics. Where appropriate, data from this study will be compared to wake studies in the literature.

Wake Measurement Objectives

The objective of the wake measurement test was to measure the average and time-varying three-dimensional velocity components in the wake of a wind turbine rotor in the locations representative of tail vane positions for small turbine rotors.

This paper describes the experimental setup used to obtain these wake measurements. Results will be presented that show rotor-dependent features of the wake and characteristics that will influence tail operation.

EXPERIMENTAL SETUP

Unsteady Aerodynamics Experiment

The measurements were made in the spring of 2000 during NREL's Unsteady Aerodynamics Experiment (UAE) in the NASA Ames Research Center 24.4-by-36.6-meter wind tunnel. One day of tunnel testing was allotted to obtain the wake measurements. More information on the UAE test program can be found at: http://wind2.nrel.gov/amestest/.

Specifications for the UAE turbine are as follows:

- Upwind operation
- 10.06-meter diameter rotor
- 0.061 rotor solidity
- 72-rpm constant rotor speed (1.2 hertz [Hz])
- Two-bladed
- Rigid rotor with 0º coning
- Rotor plane 1.40 meters upwind of yaw axis
- 12.19-meter (40-ft) hub height (tunnel centerline)

The turbine and wake measurement setup is shown in Figure 1. In this figure, the blades rotate in a counter-clockwise direction. The azimuth angle is 0º with the black instrumented blade at top dead center. The yaw direction is clockwise as viewed from the top. With the black blade at 90º azimuth (or 9 o'clock position, as shown in Figure 1), the blade tip will be pointing downwind with respect to the white blade at positive yaw.

The two wake measurement anemometers were installed on a tower 0.58 diameters (5.84 meters) downstream from the rotor plane. Anemometer 1 was the most inboard at 9% radius. Anemometer 2 was outboard 2 meters from Anemometer 1 at 49% radius. Figure 2 shows a downstream view of the anemometers. The axial (U) components of the anemometers were positioned at hub height. The two positions of the anemometers were such that the tail angle measured from the yaw axis to the center of the "U" measurement would be 6º and 29º relative to the undisturbed wind direction (see Figure 3).

For this series of tests, a yaw restraint was placed on the turbine to limit the yaw to ±65º in the event of a yaw brake failure. At +65º yaw, the rotor plane was approximately 1 foot from the outboard anemometer.

Sonic Anemometers

Two Applied Technologies Inc.[6] type K anemometers (see Figure 4) were used to acquire the wake measurements in three axes. The anemometer measures the acoustic velocity along the 15-cm path length. The instrument samples at 200 Hz, and outputs a non-overlapping block average of 20 samples at 10 Hz. The 10-Hz rate corresponded to 43.2º of rotor azimuth per average, with 8.3 averages per rotor revolution.

The two anemometers were connected to an ATI PAD-002 Data Packer. The data packer combined the anemometer outputs into a single string with no phase difference. The data packer output string was read on a

laptop computer via an RS-232 link. The laptop was used to store 30-second files, which corresponded to files acquired simultaneously with the turbine data acquisition system. The 30-second record corresponded to 36 rotor revolutions.

Test Matrix

Table 1 below shows the test matrix for wake measurement. Tunnel speed range (Uw) varied from 5 to 25 meters per second (m/s). This range corresponded to a tip-speed ratio (TSR) range of 7.5 to 1.5. The turbine yaw range varied from 0º to 60º, with higher yaw resolution between 0º and 30º. The yaw was held in position with a yaw brake. The yaw range was constrained at the higher speeds due to turbine load limits established in previous testing.

Table 1. UAE wake measurement test matrix

Uw (m/s)	TSR	Yaw Angle									
		0	5	10	15	20	25	30	40	50	60
5.0	7.5	X	X	X	X	X	X	X	X	X	X
6.0	6.3	X	X	X	X	X	X	X	X	X	X
7.0	5.4	X	X	X	X	X	X	X	X	X	X
8.0	4.7	X	X	X	X	X	X	X	X	X	X
9.0	4.2	X	X	X	X	X	X	X	X	X	X
10.0	3.8	X	X	X	X	X	X	X	X	X	X
11.0	3.4	X	X	X	X	X	X	X	X	X	X
12.0	3.1	X	X	X	X	X	X	X	X	X	X
13.0	2.9	X	X	X	X	X	X	X	X	X	X
14.0	2.7	X	X	X	X	X	X	X	X	X	X
15.0	2.5	X	X	X	X	X	X	X	X	X	X
16.0	2.4	X	X	X	X	X	X	X			
17.0	2.2	X	X	X	X	X	X	X			
18.0	2.1	X	X	X	X	X					
19.0	2.0	X	X	X	X	X					
20.0	1.9	X	X	X							
21.0	1.8	X	X	X							
22.0	1.7	X	X	X							
23.0	1.6	X									
24.0	1.6	X									
25.0	1.5	X									

Uncertainty Estimates

Estimates of the experimental uncertainty were performed using the methods outlined in AIAA S-071-1995.[7] The combined bias and precision error results are as follows:

- Wind Tunnel Velocity: ± 0.1 m/s
- Anemometer U, V, and W: ± 0.23 m/s
- Anemometer Angular Alignment: ± 1º

An additional, but unknown, uncertainty can occur in the anemometer output as a result of aliasing of the input spectrum. The ATI manual[6] describes aliasing due to the -5/3-power law of atmospheric turbulence; however, the wind tunnel and turbine wake spectrum is unknown. Therefore, the aliasing error is unknown in this application.

In addition to potential aliasing error, the anemometer has a frequency response caused by spatial averaging of the 15-cm path length and the 10-Hz block-averaging process. Due to the roll-off in the amplitude response, care needs to be exercised if the three components of wind speed are to be summed together.[8] For the purposes of this current work, the three velocity components will be reported separately.

Experimental Constraints

Listed below are constraints on the experiment resulting in differences with the normal environment of a small wind turbine.

- Inflow turbulence would not be simulated and the turbine would be fixed in yaw position. Turbines in the field are subject to atmospheric turbulence and dynamic yaw. These turbulence and dynamic yaw constraints were not considered critical because the initial model correlation would be made with steady conditions.
- The effects of the nacelle wake are unknown. The UAE nacelle has a lower frontal area compared to typical small turbine generator housings. However, the nacelle wake was deemed acceptable because all tail vanes operate within blockage of some sort.
- The effects of turbine boom components such as camera and instrumentation boxes (see Figure 1) upstream of the hub are unknown.
- The UAE turbine was designed with a limited TSR range. Small turbines can run up to a TSR of 11 at rated wind speed and when unloaded, and the wake can enter into the vortex ring state. The data from this experiment probably cannot be reliably extrapolated to higher tip-speed ratios. To address this constraint, future tests would have to be conducted with a turbine capable of higher tip-speed ratios.
- The sonic anemometers had a limited bandwidth of less than 5 Hz, with a flat amplitude response below 1 Hz. Small structures in the wake cannot be resolved with this instrument. This constraint was not considered critical because the current models only address the average wake velocity, which can be determined accurately with this instrument.

RESULTS AND DISCUSSION

Example Time Series at 0º Yaw

Figures 5 and 6 show example time series for the two anemometers at 9 m/s wind tunnel speed and 0º-yaw angle. The averages and standard deviations are shown in the plot legends. The standard deviation of Anemometer 1 (inboard) is much higher than for Anemometer 2. This unsteadiness could be a result of the nacelle wake. Also, the average of the vertical (W) component is 1 m/s for both anemometers, which shows, as expected, that the wake is rotating opposite the rotor rotation. Figure 7 shows the time series for both axial (U) velocity components at the above condition, expanded to show four seconds.

Example Spectra at 0º Yaw

Figure 8 shows power spectral densities for the above time series. Peaks occur in Anemometer 1 at the rotational harmonics up to 4/rev (at 1.2 Hz, 2.4 Hz, 3.6 Hz, and 4.8 Hz frequencies, respectively). The prominent peak is at the blade passage frequency of 2/rev or 2.4 Hz. The spectra for Anemometer #2 show prominent peaks in all velocity components at 2/rev (2.4 Hz) and a peak in the vertical (W) component at 4/rev (4.8 Hz). The 1/rev and 3/rev peaks of Anemometer 1 are not apparent in Anemometer 2.

The prominent peaks for both anemometer spectra at the 2/rev blade passage frequency may represent the passage of the shed vorticity. This periodic phenomenon was also shown in near-wake measurements conducted by Vermeer.[9] The 4/rev component might be a harmonic of coherent structures at 2/rev. Mechanical components on the instrumentation boom upstream of the rotor shown in Figure 1 are probable causes of the 1/rev (boom camera) and 3/rev (three instrumentation boxes on boom), because the 1/rev and 3/rev components do not appear in Anemometer #2's spectrum.

Wake Axial (U) Velocity at 0º Yaw

Figures 9 and 10 show the measured wake axial velocities for both anemometers at 0º yaw over the tunnel velocity range. A linear least-squares fit is shown from 10 to 25 m/s tunnel velocity. This fit illustrates a strong linear relationship between tunnel velocity and average wake velocity in this tunnel speed range.

The axial velocity standard deviation for Anemometer 2 (see Figure 10) increased substantially above 10 m/s tunnel velocity. This increase in unsteadiness was attributed to blade stall, which was confirmed in the turbine data (see Figure 11) by the abrupt increase at 10 m/s in blade flap bending moment standard deviation. Vermeer[10] also experimentally showed correlation between blade stall and wake unsteadiness.

Table 2 below shows comparisons of wake axial velocities with the data of Wentz.[11] The Wentz data is from a rotor of flat untwisted blades with a rotor solidity of 0.111. The Wentz wake measurements show a higher velocity reduction compared to the UAE data. This may be the result of lower induced effects of the optimized planform and lower solidity UAE rotor.

Table 2. Comparison to Wentz (1985) data. Radial position at 49% radius. Wentz at 0.5 diameters downstream, UAE at 0.6 diameters downstream.

TSR	Uwake/Utunnel
Wentz	Wentz
(UAE)	(UAE)
3.5	0.53
(3.4)	(0.68)
6.1	0.13
(6.3)	(0.53)

Wake Axial Induction Factor at 0º Yaw

The wake axial induction factors at 0º yaw versus TSR are shown in Figure 12 for the 0º-yaw condition. The wake induction factor was calculated by:

$$a_{wake} = 1 - (U_{wake} / U_{tunnel})$$

where:

a_{wake} = the wake axial induction factor
U_{wake} = the axial velocity of the wake
U_{tunnel} = the tunnel velocity

The wake induction factor includes the induction at the rotor ("a") and a multiplicative term for the downstream position, which is 2 for the theoretical far wake.[3] This far-wake factor is unknown for the downstream distance of this experiment. However, this factor could potentially be extracted from the turbine data by determining the induced velocity at the rotor.

The induction factor data show that the wake state was completely within the windmill operating state as shown in Yamane.[12] The relationship between axial

induction and TSR is fairly linear at both wake positions up to TSR = 3.8 (10 m/s tunnel velocity). Also, the induction factor at the inboard position shows a dip between TSR of 4 and 5. This might indicate a nacelle aerodynamic phenomenon that is dependent on Reynolds number.

Yawed Conditions

Data under yawed conditions are compared using tunnel velocities of 8 and 15 m/s. The 8m/s velocity was chosen because the rotor would be mostly unstalled. The 15 m/s condition was chosen because it was the maximum velocity that had a full yaw sweep to 60º (see Table 1). The error bars in the following figures (Figures 13, 15, 16, 18, and 19) represent one standard deviation of the data.

Yawed Conditions-- Axial (U) Velocity

Figure 13 shows the wake axial velocity versus yaw for both anemometers at wind tunnel velocities of 8 m/s and 15 m/s wind tunnel velocity. Anemometer 1 shows a sharp decline after 30º. Anemometer 2 shows a steady increase with yaw above 10º. Because the anemometer positions are fixed, the relative radial positions and downstream distances change with yaw angle. Table 3 below shows these positions normalized to the blade radius (shown schematically in Figure 14):

Table 3. Downstream distance and projected radial position from anemometers to rotor plane normalized by rotor radius (5.029 m)

	Anemometer 1		Anemometer 2	
Yaw Angle	Normalized Downstream Position	Normalized Radial Position	Normalized Downstream Position	Normalized Radial Position
0	1.16	0.09	1.16	0.49
5	1.15	0.07	1.12	0.47
10	1.15	0.04	1.08	0.45
15	1.14	0.02	1.04	0.43
20	1.15	0.00	1.00	0.42
25	1.15	-0.03	0.96	0.41
30	1.15	-0.05	0.92	0.40
40	1.16	-0.09	0.84	0.40
50	1.21	-0.12	0.73	0.43
60	1.28	-0.15	0.59	0.49

Note: Negative values in radial position represent the opposite side of the hub.

For Anemometer 2, the distance to the rotor plane decreases with increasing yaw. The relative radial position is moving inboard except at 50º and 60º yaw. Schepers[13] showed that the wake axial velocity increases with decreasing radial position for the downwind portion of a yawed rotor. Figure 13 shows an increase for Anemometer 2; however, this increase can also be attributed to closer rotor proximity resulting in a lower wake induction factor.

Yawed Conditions-- Lateral (V) Velocity

Figures 15 and 16 show the wake lateral velocity component versus yaw for 8 and 15 m/s tunnel velocities, respectively. Anemometer 2 average values are relatively low and in the positive direction as expected, because the wake should be conveyed in the direction on the side that the turbine yaws towards. The average lateral velocity at Anemometer 1, however, is negative. It is uncertain whether this is the result of the nacelle wake or the root vortex. For a tail vane in this position, the apparent angle of attack would result in a normal force towards the unfurled position. This is shown schematically in Figure 17. For the UAE turbine configuration, the tail normal force would be zero at a positive yaw offset. This result may depend on the direction of rotor rotation.

Yawed Conditions-- Vertical (W) Velocity

Figures 18 and 19 show the wake vertical velocity component versus yaw for 8 and 15 m/s tunnel velocities, respectively. Anemometer 1 is initially positive but changes sign between 20º and 30º. This result correlates well with the relative radial position found in Table 3. The radial position for Anemometer 1 crosses over to the opposite blade between 20º and 25º yaw, and the anemometer conceivably measures the root vortex rotating in the opposite direction. Anemometer 2 is positive and peaks around 30º.

Wake Unsteadiness

The small variation of wake velocity standard deviation with yaw angle suggests that the unsteadiness in the wake is unaffected by yaw angle. The majority of the variation in standard deviation is with wind speed and TSR. Also, it is uncertain what role the unsteadiness would have on the tail operation. For the measurement bandwidth of this experiment, the tail would see time-varying velocities with length scales greater than possible tail lengths. It is uncertain whether these velocity changes would be coherent in the three directions.

CONCLUSIONS

Velocity measurements in three axes were made in the wake of the 10-meter-diameter Unsteady Aerodynamics Experiment wind turbine installed in the NASA Ames 80- by 120-foot wind tunnel. Two measurement positions were chosen to represent the operating region of a small turbine tail vane.

The velocity measurements for the inboard position showed elevated unsteadiness compared to the outboard position, possibly due to the nacelle wake. The measurements showed strong dynamic components at the blade passage frequency. The unsteadiness at the outboard position showed a dramatic increase above 10 m/s tunnel velocity as a result of blade stall.

The wake axial induction factor for 0º yaw was shown to be linear with tip-speed ratio above the blade stall region (TSR < 3.8). For the entire range of measurements, the induction factor was shown to be within the windmill brake state of actuator disk momentum theory.

The behavior of the axial component under yawed conditions was difficult to attribute to any effect resulting from changes in the downwind distance and the projected radial distance along the rotor. We found that the lateral component for the inboard position had a negative value that would result in an unfurling tail normal force. The vertical component showed a reversal under yaw for the inboard position that may have corresponded to the anemometer measuring the opposing root vortex.

The unsteadiness in the measurements was found to vary little with yaw and was effected more by tip-speed ratio.

Comparison with previous wake data showed that the influence on the wake was the result of rotor planform and thus, induced effects. The turbine data from this test are currently being reduced so that the induced effects on the rotor can be determined and correlated with the wake data. The results of this work will be used to improve furling models for small turbine design and analysis.

ACKNOWLEDGEMENTS

I would like to thank my coworkers Jason Cotrell, Lee Jay Fingersh, Maureen Hand, Dave Jager, Andy Meiser, Mike Robinson, Scott Schrek, Dave Simms, and Scott Wilde, who were part of the UAE Wind Tunnel Test team. Their hard work and dedication to quality made this test campaign one of the best experiences of my career. I would also like to thank the engineers and technicians at the NASA Ames National Full-Scale Aerodynamics Complex for their helpful ideas in setting up this experiment. I would also like to credit Al Eggers of RANN Inc. for coming up with the idea for conducting this experiment in support of the Small Wind Turbine program. And finally, thanks to DOE for their continued funding support, as well as their recognition of the need for applied research to advance our knowledge of wind turbine aerodynamics.

REFERENCES

1. Forsyth, T.L., An Introduction to the Small Wind Turbine Project, in AWEA WindPower '97. 1997, American Wind Energy Association: Austin, Texas. pp. 231-239.
2. Eggers, A.J., et al., Modeling of Yawing and Furling Behavior of Small Wind Turbines, in 38th AIAA Aerospace Sciences Meeting and Exhibit 2000, American Society of Mechanical Engineers: Reno, Nevada. pp. 1-11.
3. Wilson, R.E., Aerodynamic Behavior of Wind Turbines, in Wind Turbine Technology, D.A. Spera, Editor. 1994, ASME Press: New York. pp. 215-282.
4. Ackerman, M.C., Yaw Modelling of Small Wind Turbines, in Proceedings of the European Wind Energy Conference, EWEC'91, F.J.L. Van Hulle, P.T. Smulders, and J.B. Dragt, Editors. 1991, Elsevier, Amsterdam: Amsterdam, The Netherlands. pp. 3-7.
5. Chen, D., M. Bikdash, and M. Harb, Modeling of the Autofurling Mechanism of Small Wind Turbines, in 37th AIAA Aerospace Sciences Meeting and Exhibit. 1999, American Institute of Aeronautics and Astronautics, New York: Reno, Nevada. 10 p.
6. Applied Technologies, I., Operator's Manual for a Sonic Anemometer/Thermometer: Longmont, Colorado. 47 p.
7. AIAA, Assessment of Wind Tunnel Data Uncertainty. 1995, American Institute of Aeronautics and Astronautics: Washington, DC. 84 p.
8. Wright, C.P., Applied Measurement Engineering. 1995, Englewood Cliffs, New Jersey: Prentice Hall PTR. p. 85.
9. Vermeer, N.J., Velocity Measurements in the Near Wake of a Model Rotor, in EWEC '89 European Wind Energy Conference and Exhibition. 1989, Peter Peregrinus Ltd., London, United Kingdom. pp. 532-535.

10. Vermeer, L.J. and W.A. Timmer, Identification of Operational Aerofoil State by Means of Velocity Measurements, in 1999 European Wind Energy Conference, E.L. Petersen, et al., Editors. 1999, James & James (Science Publishers) Ltd, London, UK: Nice, France. pp. 168-171.
11. Wentz, W., et al., Horizontal Axis Wind Turbine Wake and Blade Flow Studies from Model Tests, in The Eighth Annual Energy-Sources Technology Conference and Exhibition, A.H.P. Swift, Editor. 1985, The American Society of Mechanical Engineers, New York: Dallas, Texas. pp. 235-244.
12. Yamane, T., Y. Tsutsui, and T. Orita, The Aerodynamic Performance of a Horizontal-Axis Wind Turbine in Large Induced-Velocity States, in Fourth International Symposium on Wind Energy Systems. 1982, BHRA Fluid Engineering, England: Stockholm, Sweden. pp. 85-100.
13. Schepers, J.G., An Engineering Model for Yawed Conditions, Developed on Basis of Wind Tunnel Measurements, in 37th AIAA Aerospace Sciences Meeting and Exhibit. 1999, American Institute of Aeronautics and Astronautics, New York: Reno, Nevada. pp. 164-174.

FIGURES

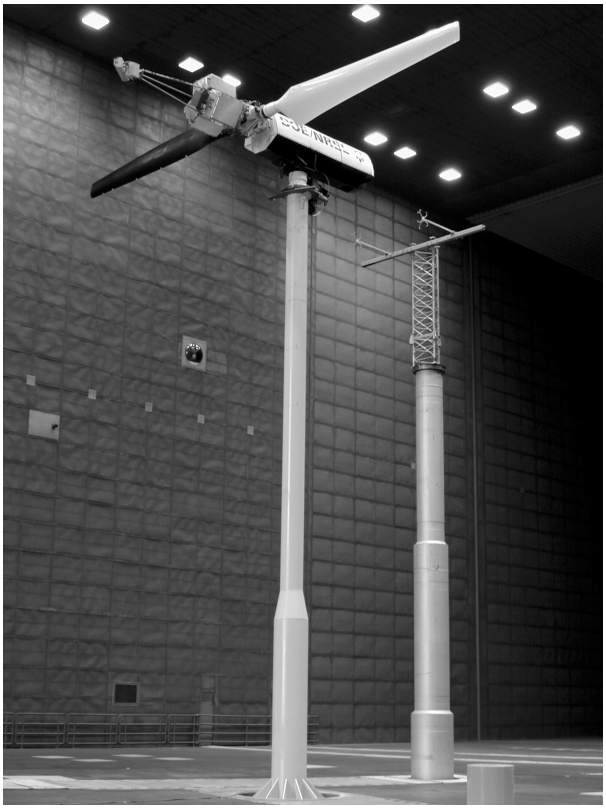

Figure 1. UAE Turbine with downwind wake measurement installation in 80- by 120-foot wind tunnel

Figure 2. Downstream view of wake measurement tower. The turbine in this photo represents the downwind configuration at 180º yaw. The upwind turbine configuration is shown in Figure 1.

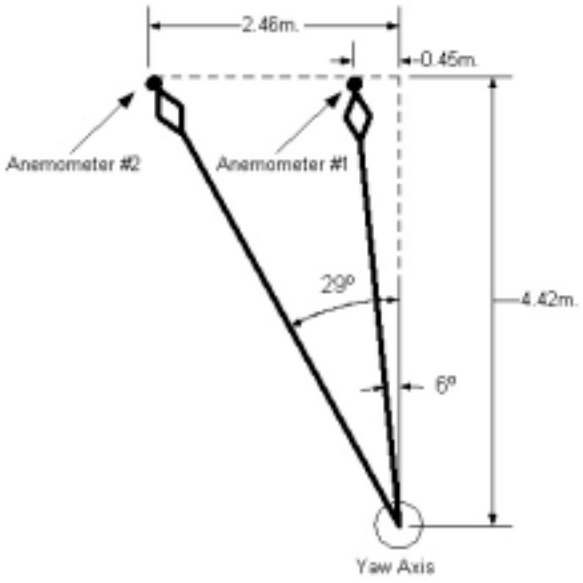

Figure 3. Tail angles based on distance from yaw axis to anemometer positions

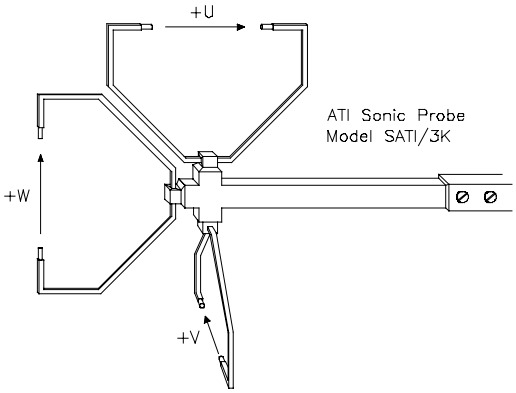

Figure 4. ATI Sonic Probe

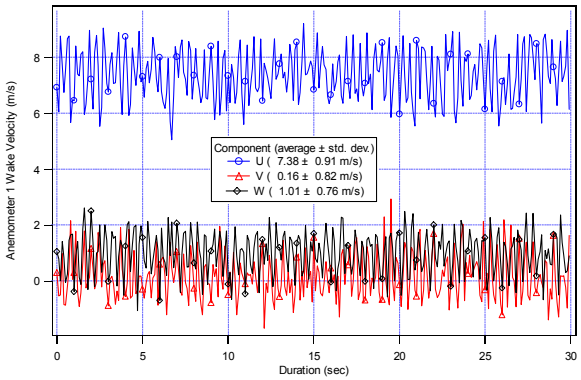

Figure 5. Anemometer 1 (inboard) time series at 0º yaw, 9 m/s tunnel speed

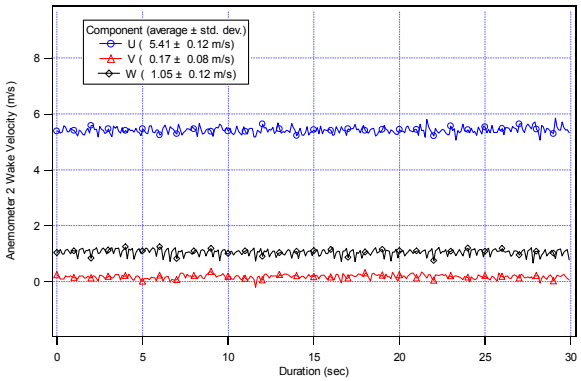

Figure 6. Anemometer 2 (outboard) time series at 0º yaw, 9 m/s tunnel speed

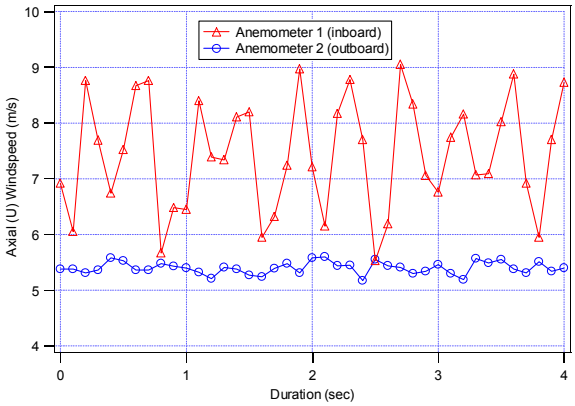

Figure 7. Expanded time series for axial (U) component at 0º yaw, 9 m/s tunnel speed

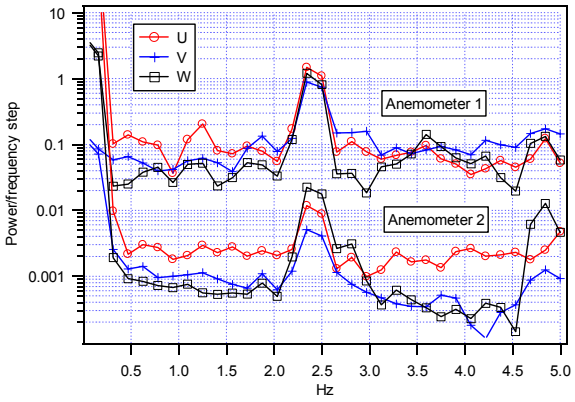

Figure 8. Power spectral density for the time series at 0º yaw, 9 m/s tunnel speed. 64 segments, Hanning window applied.

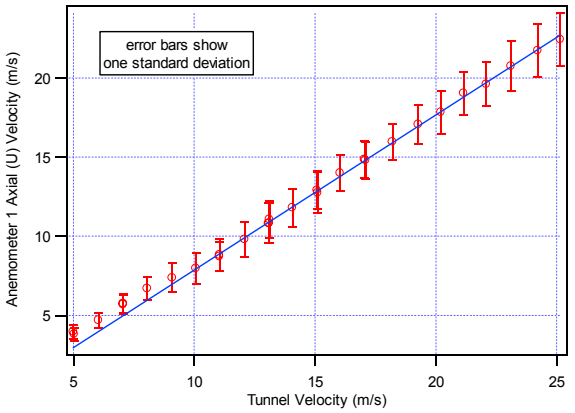

Figure 9. Anemometer 1 axial velocity and standard deviation versus tunnel wind speed.

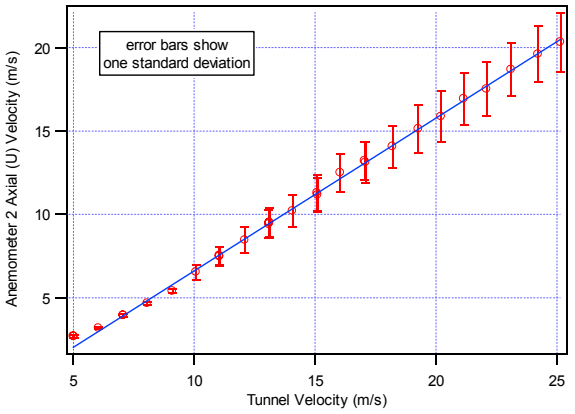

Figure 10. Anemometer 2 axial velocity and standard deviation versus tunnel wind speed.

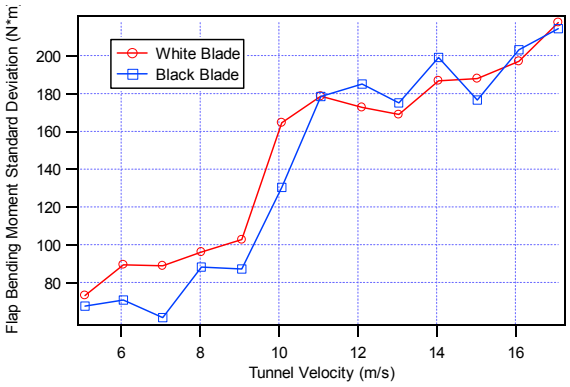

Figure 11. Standard deviation of blade flap bending moment versus tunnel wind speed.

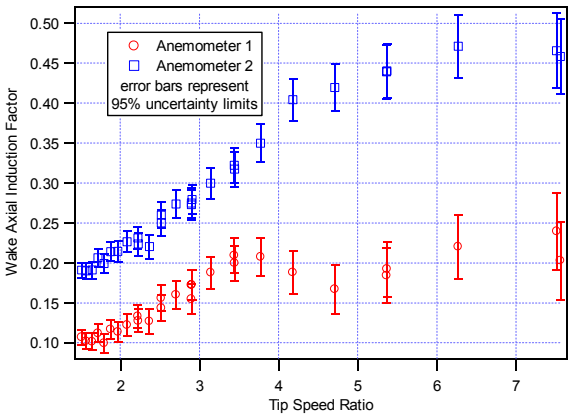

Figure 12. Total axial induction factor versus TSR at 0º yaw.

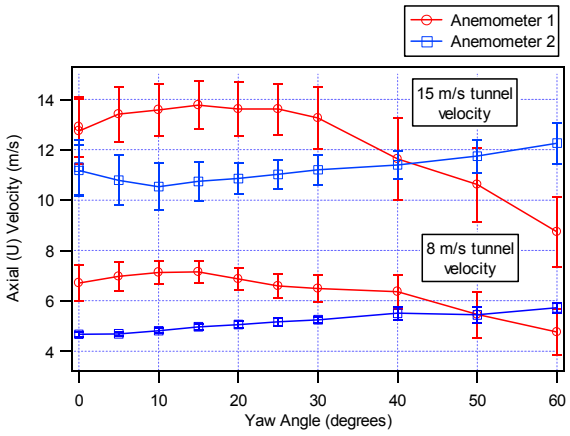

Figure 13. Wake axial (U) velocity versus yaw at 8m/s and 15 m/s tunnel velocity.

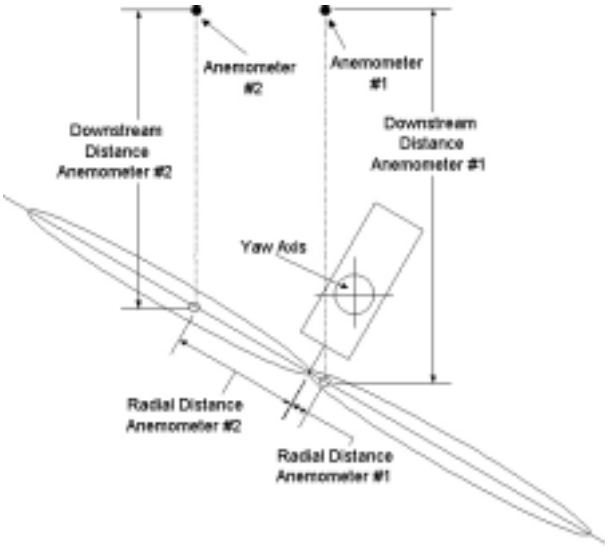

Figure 14. Definition of anemometer downstream and radial distances with the turbine at 30º yaw.

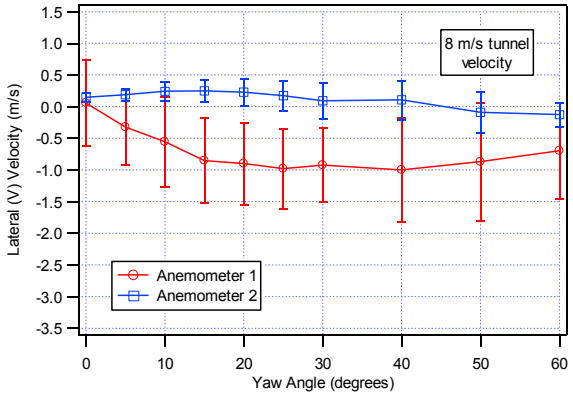

Figure 15. Wake lateral (V) velocity versus yaw at 8 m/s tunnel velocity.

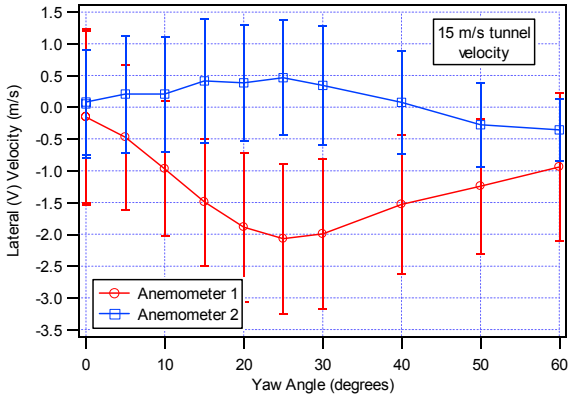

Figure 16. Wake lateral (V) velocity versus yaw at 15 m/s tunnel velocity.

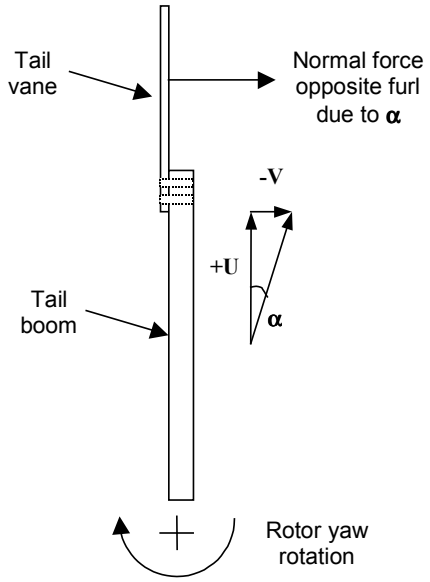

Figure 17. Negative lateral velocity resulting in tail unfurling normal force.

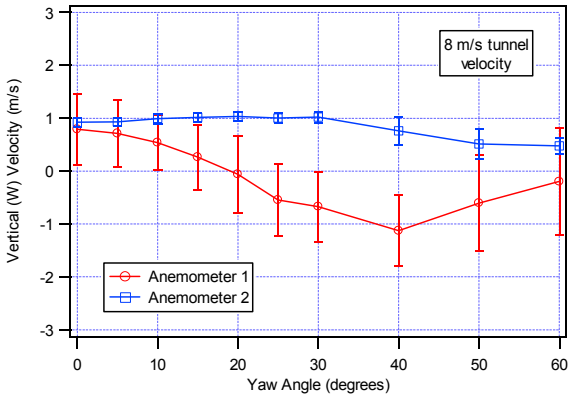

Figure 18. Wake vertical (W) velocity versus yaw at 8 m/s tunnel velocity.

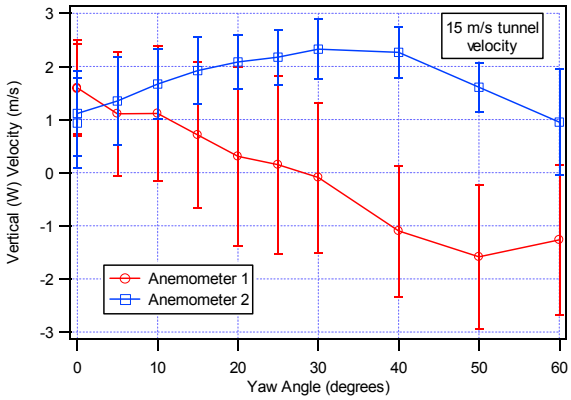

Figure 19. Wake vertical (W) velocity versus yaw at 15 m/s tunnel velocity.